Geomechanics and Engineering, *Vol. 40, No. 3 (2025) 205-216*
https://doi.org/10.12989/gae.2025.40.3.205

Innovative numerical techniques for calculating rock strength characteristics: Leveraging integrated machine learning and geostatistical methods

Fataneh Fakhri[1], Danial Mansourian[2], Hossein Baghishani[1], Ayub Elyasi*[3], Esmael Makarian[4] and Fatemeh Saberi[5]

[1]*Department of Statistics, Shahrood University of Technology, Shahrood, Iran*
[2]*Mewbourne College of Earth and Energy, Oklahoma University, USA*
[3]*Department of Petroleum Engineering, College of Engineering, Knowledge University, Erbil 44001, Iraq*
[4]*Department of Mining Engineering, Sahand University of Technology, Tabriz 94173-71946, Iran*
[5]*Harold Hamm School of Geology & Geological Engineering, University of North Dakota, USA*

(*Received June 22, 2024, Revised January 27, 2025, Accepted February 3, 2025*)

Abstract. Accurately predicting rock mechanical properties, such as uniaxial compressive strength (UCS) and internal friction angle (φ), is crucial for various subsurface engineering applications. Traditional laboratory testing methods for determining these parameters are often expensive and time-consuming. This research presents a novel methodology that integrates two key techniques, machine learning (ML) and geostatistics, to more efficiently and accurately estimate UCS and φ from routinely measured P- and S-wave velocities (VP and VS) based on well-logging operations. The methodology involves training three machine learning models, including multivariate adaptive regression splines (MARS), least absolute shrinkage and selection operator (Lasso), and Ridge regression, on 70% of the data to predict UCS and φ. Predictions were validated through cross-validation on the remaining 30% of the data. Next, the Ordinary Kriging (OK) method was employed to evaluate the accuracy and robustness of the applied methods. Finally, all the results were assessed using various metrics, including mean biased prediction error (MBPE), mean absolute prediction error (MAPE), mean squared prediction error (MSPE), and R-squared (R^2). The results indicate that the Ridge model delivers the best performance for predicting φ, with the lowest MSPE of 2.29 and the highest R^2 of 0.98. Additionally, the value of MAPE is the lowest at 0.91, and MBPE has the lowest distance to zero. For UCS, the MARS demonstrates the lowest MSPE and MAPE values, as well as the highest R^2, indicating superior performance compared to the other models.

Keywords: geostatistics; internal friction angle; machine learning; seismic velocities; uniaxial compressive strength

1. Introduction

Accurately estimating geomechanical parameters is essential for a wide range of subsurface studies, including civil engineering, mining projects, and oil and gas surveys (Shouri *et al.* 2024, Hashemi *et al.* 2024). Key geomechanical parameters, such as uniaxial compressive strength (UCS) and internal friction angle (φ) play a critical role in developing effective and safe strategies for exploration and drilling, helping to prevent unforeseen and hazardous events, such as eruptions.

The process of acquiring rock cores from boreholes for laboratory testing is highly costly, and the expenses associated with the geomechanical laboratory tests can further limit their feasibility. Additionally, the coring process and the maintenance conditions of the core samples prior to testing can compromise sample quality, negatively affecting the accuracy of the results as environmental factors, such as fluctuations in moisture and temperature, can exacerbate these inaccuracies and errors. Furthermore, deriving strength properties from well logs based on empirical correlations with other fields, particularly in the absence of adequate calibration, may yield misleading results.

Estimating these parameters is also beneficial for wellbore integrity studies, the construction of 3D and 4D geomechanical models. Studies have demonstrated that accurate estimation of these factors is crucial for enhancing productivity and recovery factors in the development plans of oil and gas reservoirs. For instance, in wellbore stability analysis, enhanced oil recovery (EOR) projects, and storage initiatives, it is essential to analyze rock strength properties. This analysis allows for the assessment of stress alterations resulting from drilling activities or changes in fluid pressure and temperature on both the reservoir and surrounding rocks (Goshtasbi *et al*. 2013, Saberi *et al*. 2024, Elyasi *et al.* 2016). Geomechanical attributes play a vital role in improving project outcomes; thus, understanding and estimating parameters related to rock mechanics and fluid-induced pressure are critical for the effective characterization and management of reservoirs (Makarian *et al.* 2023a, Larki *et al*. 2023).

This study aims to present an optimal method for estimating UCS and φ. By leveraging digital rock mechanics and advanced technologies such as machine learning (ML), the research seeks to generate new insights

*Corresponding author, Ph.D.
E-mail: a.elyasi1986@yahoo.com

ISSN: 2005-307X (Print), 2092-6219 (Online)

and apply often-overlooked numerical methods, like geostatistics, to enhance estimation processes. The proposed approach integrates ML and geostatistics to efficiently estimate UCS and φ using only two seismic datasets, ensuring that the method is fast, reliable, and cost-effective. In light of the preceding researches, there is a significant need to establish mathematical equations that correlate seismic parameters with rock mechanics properties. This study offers essential insights that can be applied to other similar projects or studies.

1.1 Internal friction angle (φ)

The internal friction angle (φ) is a fundamental mechanical parameter used to evaluate soil and rock's strength and failure characteristics. This angle represents the minimum angle of inclination required to induce the sliding of a block of equivalent material resting on a surface (Hudson and Harrison 2000). It is a direction-dependent parameter ranging from 0 to 90 degrees and is crucial in the stress-strain behavior of materials under pressure (Khalifeh-Soltani *et al.* 2021, Wang and He 2023). The internal friction angle is affected by various factors, comprising the particle size, orientation of layering planes, pore water pressure, and particle shape (Hudson and Harrison 2002).

The internal friction angle is determined through laboratory tests such as triaxial or direct shear tests, as well as by developing Mohr's circles or linear fits of the Hoek-Brown failure envelope (Karev et al. 2020; Villeneuveα and Heap 2021). The Mohr-Coulomb combination visually represents the relationship between the shear and normal stress at failure (Zoback and Kohli 2019). Developing Mohr's circles is crucial in determining the strength of rocks and other materials (Fig. 1).

By providing the friction coefficient and the angle of internal friction, these circles are constructed for each specimen to assess the shear stress and the strength chart of rocks (Tsoi and Usol'tseva 2019, Xu and Jin 2024). The most common way of determining the shear stress of materials is lab measurements where the Mohr-coulomb criterion is derived from laboratory triaxial deformation

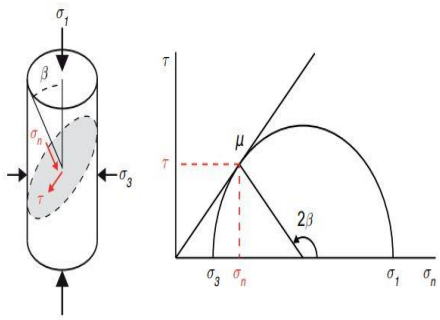

Fig. 1 Coulomb theory. (a) A plane with angle β to the maximum stress σ1 will slip at a ratio of shear stress (τ) to normal stress (σn) defined by the coefficient of friction μ. (b) A 2D Mohr circle depicts the shear and normal stress values at which frictional failure occurs (Zoback and Kohli 2019)

laboratory information (σ1 > σ2, and σ2= σ3, where the notations σ1, σ2, and σ3 denote the maximum, intermediate, and minimum principal stresses, respectively (Eq. (1)) (Labuz and Zang 2012).

$$\tau = c' + \sigma' \tan\varphi'_f \quad (1)$$

where τ is the shear strength at effective confining pressure σ', c' is the cohesion, and φ_f is the internal friction angle.

The internal friction angle is also a critical parameter for characterizing the brittleness of rocks and determining their strength (Elyasi and Goshtasbi 2015, Zhang *et al.* 2016, Hernomita and Erfando 2023). However, the internal friction angle tends to decrease with increasing confining pressure, which may limit its use as a measure of brittleness (Zhou *et al.* 2018). Zhou et al. conducted tests on various types of sandstone and marble to address this issue. They proposed a novel brittleness index (Bi) incorporating additional factors such as the ratio of elasticity modulus to post-peak modulus and the ratio of post-peak stress drop to peak stress. They found that Bi generally decreased with increasing confining pressure and exhibited a linear correlation with φ for black and red sandstone but an exponential relationship for marble.

Laboratory tests such as triaxial and direct shear are the conventional approaches for measuring a material's internal friction angle and shear strength. However, numerical and modeling techniques have extended their reach to assess materials' shear stress and strain, such as the finite-discrete element method (FDEM) (Munjiza 2004, Liu *et al.* 2016). Min *et al.* (2020) employed the FDEM approach to simulate the shear strength of the direct shear test and analyzed the impact of friction coefficient and bulk friction angle of rock joints. Tsoi and Usol'tseva (2019) opted for a mathematical methodology to present formulas for determining internal friction cohesion coefficients and angles for a linear and nonlinear envelope type of Mohr-Coulomb circles. Zegzulka *et al.* (2022) developed a modeling approach to construct a comprehensive model that accounts for the internal friction angle of particles while being independent of particle size. Their proposed model enabled the interpretation of internal friction angle measured values and facilitated the simulation of probably measured values.

In a recent study, Dong *et al.* (2022) employed the particle flow code (PFC) as an alternative method to simulate the cohesion and friction between mineral particles in rocks at the mesoscale level. The authors utilized a two-dimensional PFC (PFC2D) calculation program to perform a numerical direct shear test on the structural planes of a rock mass. The study investigated the failure characteristics of the planes under varying undulant angles of 10, 20, and 30 degrees and normal stresses. In another study, Zegzulka *et al.* (2022) developed a model that established a correlation between the shape of the angle of internal friction for particles and the angle of internal friction of particles during steady flow. The authors confirmed the validity of their model through experimentation.

As explained before, estimating the internal friction angle of rocks is crucial in geomechanics. Still, it can be challenging and time-consuming due to the complex testing process and the large amount of data to be analyzed. As

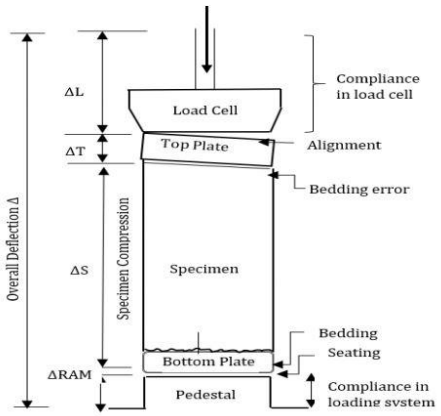

Fig. 2 Sources of error in UCT (Isah *et al.* 2020)

discussed in the following, machine learning presents a potential solution to these challenges. By analyzing vast amounts of data and identifying patterns, machine learning models can enhance the accuracy and reliability of internal friction angle estimates.

1.2 Uniaxial Compressive Strength (UCS)

Accurately determining uniaxial compressive strength (UCS) is critical for various rock mechanical-related activities, such as building geomechanical models. It characterizes the maximum compressive stress a rock can withstand without failure during uniaxial loading. It is essential to comprehend the mechanical features of rocks in the fields of study and practice that involve using natural resources and materials, such as rocks, for various purposes (Elyasi *et al.* 2023, Karaman 2024). Examples of these fields include civil engineering infrastructure design, mining engineering mineral extraction, and petroleum engineering oil and gas exploration and production. Various methods, including laboratory testing, have been widely investigated to achieve this understanding (Isah *et al*. 2020).

Recent studies by Abdullah *et al.* (2023), Abd El Aal *et al.* (2025), and Al-Homidy *et al*. (2024) underscore the importance of UCS in geotechnical applications. Abdullah *et al.* (2023a) focus on geotechnical parameters for historical buildings in Najran City, while Abd El Aal *et al*. (2025) identify depth variations as indicators of UCS in Najran granites, highlighting their relevance in complex terrains. Additionally, Abdullah *et al*. (2023b) explore how Coarse Aggregate Crushing Waste (CACW) can enhance UCS and reduce carbon footprints, and Al-Homidy *et al.* (2024) examine the effects of cement kiln dust on the properties of sand dunes, further demonstrating UCS's role in ensuring material durability and stability in arid environments.

The uniaxial compression test (UCT) developed by the International Society for Rock Mechanics (ISRM) is the standard laboratory technique for investigating the mechanical properties of rocks. During the test, a cylindrical rock sample two to three times longer than its diameter is subjected to induced strain beyond normal. The load is gradually increased until the sample fails. Stress-strain data is collected to generate the stress-strain curve of the rock sample and calculate various parameters such as uniaxial (unconfined) compressive strength, Young's modulus (E), and Poisson's ratio (v) (Culshaw 2015, Lee *et al.* 2024). Nonetheless, this method only measures the specimen's length change and not all other elastic components of the testing apparatus. Therefore, it considers any slippage of the sample within the grips and any roughness or unevenness on the sample surfaces, resulting in an overestimation of the strain values due to errors related to bedding and system compliance. The outcome of this could result in an incorrect calculation of Young's modulus, Poisson's ratio, and even uniaxial compressive strength. Fig. 2 illustrate the sources of error associated with this laboratory method.

Due to the challenges associated with sampling, expensive operational procedures, and inaccuracies, other techniques, such as well logging and real-time drilling attributes, have gained popularity. Gao *et al*. (2021) proposed a concept for predicting rock UCS using digital core drilling to address the challenge of obtaining real-time UCS data for rocks at engineering sites. Faradian *et al.* (2022) employed non-destructive and indirect testing methods, such as measuring the P-wave velocity (Vp) and Schmidt hammer rebound (SHR), as a substitute for predicting UCS. Sadeghi *et al*. (2022) also employed a comparable approach by establishing a link between UCS and various factors such as point load index (PLI), Schmidt hammer rebound (SHR) value, and Brazilian tensile strength (BTS) to forecast the values of uniaxial compressive strength based on the young modulus (UCS-E) and sample size factors such as length-to-diameter ratio (L/D) and volume.

The research introduces several novel contributions across various aspects, which will be elaborated upon in detail in the following sections. The first novelty is related to the input data. Through calculating indirect ways in both target parameters, no special attention is paid to employing only seismic velocity data, especially in friction angle prediction. This is because indirectly calculating φ is challenging due to material variability, scale dependence between lab and real-world results, inconsistent environmental testing conditions, complex stress states, the influence of fractures, and insufficient correlations between indirect measurements and φ.

Regarding the studies, seismic velocity data are reliable indicators of rock mechanical properties, making them an ideal data source for predicting UCS and φ. This research utilized only seismic velocities, including P and S wave velocities, as two standard seismic tools often measured in almost all underground surveys to calculate UCS and φ. Therefore, this method provides all engineers and researchers with fast and cost-effective estimation; however, previous studies usually use laboratory information to predict φ, which is expensive and time-consuming. Additionally, in some situations, providing the needed materials for laboratory settings such as core is difficult or impossible, for example, in weak formations or deviation wells. Besides, those previous studies that wanted to calculate the target parameters indirectly utilized at least

five or six imputes. However, this study generated a new insight for calculating UCS and φ by standard, reliable, available, and at least input information. Another aspect of the data that enhances the quality of the research is that the target parameters (UCS and φ) were correlated with laboratory results, leading to the most reliable results.

An additional innovation pertains to the application of numerical methods. This study introduces novelties by integrating multiple machine learning and geostatistics modeling approaches, including MARS, Lasso, Ridge, and Kriging, to create a comprehensive framework for estimating UCS and φ using only P and S wave seismic velocities. For the first time, this research uses these types of ML methods; however, the previous studies utilized artificial neural networks (ANN), support vector machines (SVM), or deep learning. The ML methods offer several advantages, particularly in simplicity and interpretability. MARS provides piecewise linear relationships that are easier to understand than more complex models, while Lasso performs variable selection by shrinking some coefficients to zero, effectively highlighting significant predictors. Ridge retains all predictors but balances their coefficients to prevent overfitting. These methods generally require less data to achieve good performance compared to ANN and deep learning, and they incorporate regularization techniques to manage multicollinearity and enhance robustness in smaller datasets. Additionally, they boast faster training times and involve fewer hyperparameters, simplifying the modeling process. Lasso is especially effective in high-dimensional spaces, maintaining model simplicity when the number of predictors exceeds observations.

Moreover, this research employs geostatistical methods to calculate the target parameters, which were not considered in the previous study. Another novelty of the research is employing simultaneous ML and geostatistics approaches. Robust cross-validation enhances the reliability and generalizability of predictions, while MARS and Lasso effectively identify significant variables, improving interpretability and efficiency.

This research has several merits. It highlights the flexibility of MARS in capturing complex, non-linear relationships between seismic data and rock mechanical properties. Lasso and Ridge regression effectively manage multicollinearity and reduce overfitting, ensuring model robustness. Additionally, Kriging provides valuable spatial predictions and uncertainty estimation in geological contexts. Overall, these methods significantly enhance the accuracy of UCS and φ estimates compared to conventional techniques, leading to a fast, reliable, and cost-effective prediction.

One of the most essential merits and novelties of the research is that the research provides intelligent mathematical relationships among the input information and target parameters, which none of the pervious study addres to it.

On the other hand, this study has some limitations that should be mentioned. The accuracy of the methods used in this study is highly dependent on the quality and representativeness of the input seismic data, as poor data can lead to inaccurate predictions. While adaptive methods like MARS effectively model complex relationships, they may pose interpretability challenges. Additionally, Kriging's assumption of stationarity may limit its applicability in varied geological settings. Finally, methods such as MARS and Kriging can be computationally intensive, requiring robust hardware and longer processing times for larger datasets.

Overall, this study provides a novel and effective approach to predicting UCS and φ of rocks, which can have significant implications for various fields that rely on accurate predictions of rock mechanical properties. The approach also highlights the potential of ML and Geostatistics methods for improving the accuracy and efficiency of predicting rock mechanical properties with at least data.

2. Data description

Petrophysical Log data plays a crucial role in geomechanical evaluation, and it can be acquired using wireline tools or logging while drilling (LWD) tools. P-wave and S-wave velocities are commonly used to characterize the petrophysical properties of rock formations employed to extract parameters related to rock mechanics features (Makarian *et al.* 2023b). The necessary editing and correction, such as depth matching, merging, despiking, environmental correction, etc., was applied to prepare these two raw logs for the geomechanical calculations. Any unreliable data, such as cycle skips on the sonic log or hole washouts, are rectified.

Furthermore, any environmental factors that could affect the data, such as wellbore caving, mud salinity, mud pressure, and mud cake, were also adjusted. In order to ascertain the strength-physical property relationships within this particular field, a comprehensive analysis was conducted to establish the correlations between mechanical properties derived from core laboratory tests and log data. It is important to highlight that these results were meticulously calibrated, ensuring a high level of accuracy and reliability. By rigorously calibrating the strength parameters, we can confidently establish the relationships between mechanical properties and effectively utilize this information for further analysis and decision-making processes. Fig. 3 illustrates the depth profile of the compressional and shear wave velocities and the formation strength parameters (φ, UCS) obtained from strength-physical property relationships. These data were used as inputs for subsequent machine learning and geostatistical evaluations.

3. Proposed methodology

3.1 General spatial modeling and prediction

Here, we use a general framework for spatial modeling through a random process. Let $Y_m(\mathrm{x}_\cdot)$ denote a real-valued spatial process in d dimensions where $\mathrm{x}_\cdot$ is the location of the process $Y_m(\mathrm{x}_\cdot)$ varying over the index set D, a subset of $\mathbb{R}^d$. The spatial process $Y_m(\mathrm{x}_\cdot)$ can be decomposed into a

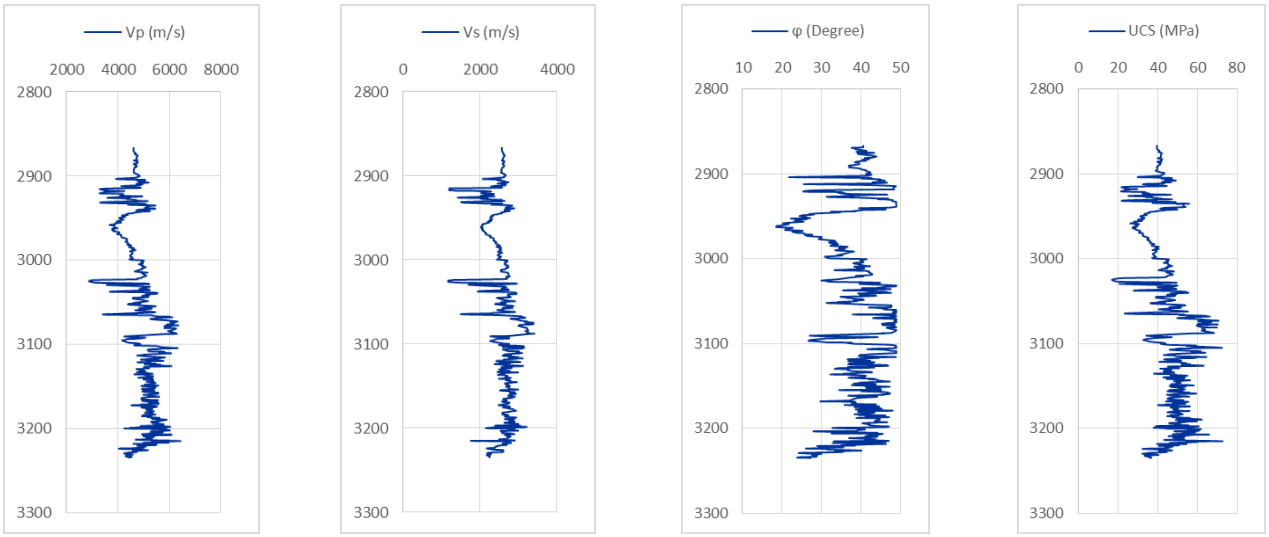

Fig. 3 Depth profile of all the used data in the study

deterministic location-dependent component, $f_m(\mathrm{x})$, called the trend and two random components measuring spatially correlated variations, $\delta_m(\mathrm{x})$, and non-spatial measurement errors (the nugget effect), $\varepsilon_m(\mathrm{x})$, respectively (Chilès and Delfiner 2012). Therefore, we have (Eq. (2)).

$$Y_m(\mathrm{x}) = f_m(\mathrm{x}) + \delta_m(\mathrm{x}) + \varepsilon_m(\mathrm{x}). \quad (2)$$

The trend component represents the behavior of the process at a large scale, whereas the spatial component represents the local small-scale variability. Moreover, it is usually assumed that the two random components are uncorrelated, and $\delta_m(.)$ is a zero-mean stationary Gaussian process (Cressie 1991).

The spatial prediction of the response variable, $\hat{Y}$, in a new location ($\mathrm{x}_{\mathrm{new}}$) can be expressed as follows (Eq. (3)).

$$\hat{Y}_m(\mathrm{x}_{\mathrm{new}}) = \hat{f}_m(\mathrm{x}_{\mathrm{new}}) + \hat{\delta}_m(\mathrm{x}_{\mathrm{new}}) \quad (3)$$

Where $\hat{f}_m(\cdot)$ is the trend function estimate, and $\hat{\delta}_m(\cdot)$ is the prediction of the small-scale spatial process based on (ordinary) Kriging the detrended data (Cressie 2015). Ordinary Kriging (OK) on residuals (detrended data) is straightforward and can be easily implemented today using standard software packages (Hengla *et al.* 2007). Hence, efficient trend modeling plays an important role in having an accurate spatial prediction of the response variable. Both over-fitting and under-fitting the trend could result in non-desirable inferences and predictions. The following section will apply three popular machine-learning techniques to model the trend function.

3.2 Trend modeling

In our application, we assume $\mathrm{V_P}$ and $\mathrm{V_S}$ determine the trend function of the response variable, i.e., (Eq. (4)).

$$f_m(\mathrm{x}) = g_m\big(V_P(\mathrm{x}), V_S(\mathrm{x})\big) \quad (4)$$

Where $g(\cdot\,,\cdot)$ can be a general bivariate function, including linear and nonlinear. If a linear model is reasonable, then $f_m(\mathrm{x}) = \beta_0 + \beta_1 \mathrm{V_P}(\mathrm{x}) + \beta_2 \mathrm{V_S}(\mathrm{x})$ in which β_0 is the intercept and (β_1, β_2) are regression coefficients that measure the linear effects of $\mathrm{V_P}$ and $\mathrm{V_S}$. It must be mentioned that the hypothesis of the equation is supported by the scatter plots presented in Fig. 4, which illustrate a significant linear and potentially nonlinear relationship between the variables $\mathrm{V_P}$ and $\mathrm{V_S}$ and the variations in the response variables. The observed patterns in the plots suggest that these predictor variables are integral to modeling the trend function of the response variable. We can perform an exploratory data analysis to determine whether linearity could be appropriate. Fig. 4 shows the scatter plots of different response variables, ϕ and UCS, against $\mathrm{V_P}$ and $\mathrm{V_S}$. There is evidence of some possible nonlinear relationships between $\mathrm{V_P}$ or $\mathrm{V_S}$ and response variables to some extent. Applying a linear model could lead to inaccurate trend estimates in this case. We can use the general form of (4) to relax the assumption of a linear trend in a nonparametric regression framework. Nevertheless, the curse of dimensionality could affect trend modeling in such situations. Additive models (Friedman and Stuetzle 1981) are considered to avoid this problem, in which the trend function is defined as (Eq. (5)).

$$f_m(\mathrm{x}) = g_1\big(V_P(\mathrm{x})\big) + g_2\big(V_S(\mathrm{x})\big) \quad (5)$$

Where g_1 and g_1 are unknown smooth functions estimated from the data. As part of our proposed techniques, we will consider this view of trend modeling.

Fig. 4 also displays the scatter plot of $\mathrm{V_P}$ against $\mathrm{V_S}$. There is a strong linear relationship between these two predictors. Their correlation coefficient is equal to 0.851. Therefore, it appears that the two variables are highly collinear. To assess collinearity formally, we used the variance inflation factor (VIF) criterion, which is VIF=3.631 for these two predictors. VIFs greater than 2.5 are significant (Johnston *et al.* 2018). To neutralize collinearity, trend modeling strategies should consider this feature as well. Shrinkage methods such as Ridge regression and Lasso (Hastie *et al.* 2009) could be used to achieve this goal.

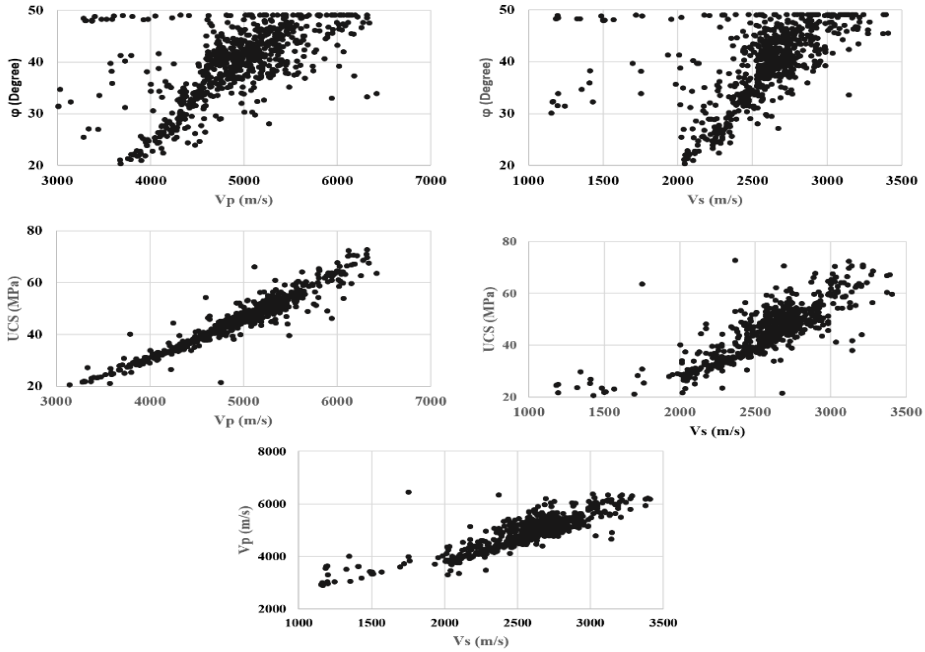

Fig. 4 Scatter plots of the target variables versus V_P and V_S and scatter plots of the V_S against V_P

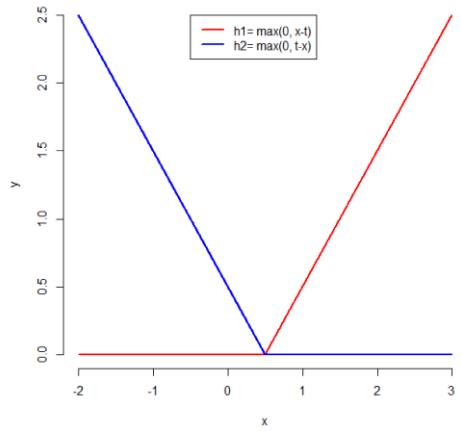

Fig. 5 The basic functions for observing t = 0.5 are shown in the image in red and blue h_1= max (0, x-t) and h_2=max(0, t-x)

3.3 MARS method

The Multivariate Adaptive Regression Splines (MARS) method is a nonlinear nonparametric regression model Fridman developed in 1991. This method is a generalization of the Spline approach and is usually used for multivariable datasets on large scales. A two-stage (Forward and backward) approach follows a simple calculation method. MARS equation is as follows (Eq. (6)) (Hastie *et al*. 2009).

$$f(x) = \beta_0 + \sum_{k=1}^{K} \beta_k h_k(x) \tag{6}$$

Where β_0 is the intercept and β_k is the regression coefficient calculated using the squared of the residuals. h_k is a linear basis function subset of (Eq. (7)).

$$S = \{(x_j - t)_+, (t - x_j)_+\} \tag{7}$$

Where $(x_j - t)_+ = \max(0, x_j - t)$ and $(t - x_j)_+ = \max(0, t - x_j)$. so that $t \in \{x_{1j}, x_{2j}, \dots, x_{nj}\}$ is knot and $j = 1, \dots, P$ is several variables, and n represents the sample size. In Fig. 5, the basis function for t = 0.5 is illustrated.

MARS automatically selects variables and values of those variables for knots of the functions. This method uses a generalized cross-validation (GCV) approach, which can be written as follows (Eq. (8)).

$$GCV_m = \frac{SSE_m}{\left(1 - \frac{(\eta K_m + 1)}{n}\right)^2} \tag{8}$$

Where the SSE_m is the sum of the squared error of model m, K_m is the number of basic functions of the model m, η is the smoothing parameter, and n is the number of observations. In other words, by utilizing the GCV, MARS benefits from a more efficient and rapid calculation technique.

3.4 Shrinkage methods

While modeling the process between the data, choosing the correct variable and estimating the best regression coefficient carries a significant weight. Collinearity in explanatory variables can become troublesome as it will increase the regression coefficients. The shrinkage methods suppress this issue by limiting the variations of the regression coefficients and reducing the predictive variance and the square of errors. However, using this method leads

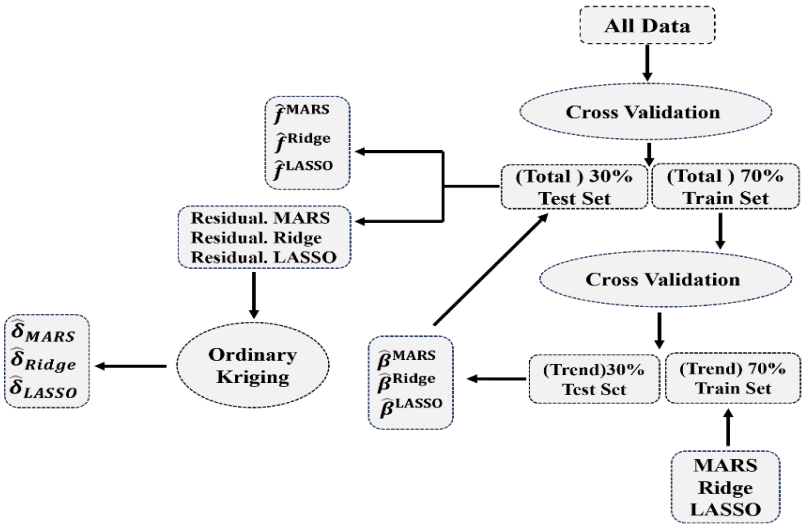

Fig. 6 Flowchart for the proposed advanced numerical method for UCS and φ

to the Bias of the estimators. Many of these methods reduce the negative impact of the collinearity problem by variable selection. The Ridge approach is one of the Shrinkage methods that improve the regression model despite the collinearity and without removing the explanatory variables (McDonald 2009). Ridge method minimizes the estimation of the sum of squared errors by applying a condition given in Eqs. (9) and (10).

$$\hat{\beta}^{\text{Ridge}} = \underset{\beta}{\operatorname{argmin}} \sum_{i=1}^{N} \left(y_i - \beta_0 - \sum_{j=1}^{P} x_{ij}\beta_j \right)^2 ; \quad s.t \sum_{j=1}^{P} \beta_j^2 \le t. \tag{9}$$

Where $t \ge 0$ is the tuning parameter and $\lambda \ge 0$ is the penalty factor that controls the amount of shrinkage of penalty estimates; also, t and λ be had one-to-one correspondence. If λ equals zero, no penalty is applied, and the ordinary least square (OLS) estimator is obtained. When it tends toward infinity, some of the regression coefficients become near zero, but they will never be equal to zero. Because the Ridge method is not a subset selection method.

The Lasso (Least Absolute Shrinkage and Selection Operator) approach is similar to the Ridge method, with the difference that in the Ridge method, the term of the penalty should be $\sum_{j=1}^{P} |\beta_j| \le t$. In this method, when the penalty factor tends to infinity, some coefficients may become zero, and some variables are removed from the model (Hastie *et al.* 2009).

$$\hat{\beta}^{\text{Ridge}} = \underset{\beta}{\operatorname{argmin}} \{ \frac{1}{2} \sum_{i=1}^{N} \left(y_i - \beta_0 - \sum_{j=1}^{P} x_{ij}\beta_j \right)^2 + \lambda \sum_{j=1}^{P} \beta_j^2 \}. \tag{10}$$

4. Model selection

In many scientific studies, the analyst faces various explanatory variables, amongst which they must pick a limited number according to the project requirements. This happens as if the model contained unnecessary and unimportant variables; it will suffer from overfitting (Min *et al.* 2024). In addition, interpreting such models is difficult; hence, collecting observations will become time-consuming and costly. On the contrary, if the model goes through the process of underfitting, the resulting model may not fit and explain the existing data (Cressie and Moores 2022, Makarian *et al*. 2023c, Mirhashemi *et al*. 2022). Finding a model unaffected by over-fitting and under-fitting phenomena Falls within the variable selection process. Thus far, various statistical methods have been proposed to select the model, comprising Akaike Information Criterion (AIC), Bayesian Information Criterion (BIC), and adjusted R^2 (R^2_{adj}) (James *et al*. 2013).

4.1 Cross-Validation (CV)

Not every model selection criterion can check the predictive accuracy of the model. For example, the value of the R^2 variable does not necessarily equal a good-fitting model. Because of the increasing explanatory variables, more information has been entered into the model, which leads to a possible over-fitting of the data. This is one of the defects of this criterion.

Cross-validation (CV) is a statistical learning technique used to assess the predictive capability of a statistical model, particularly in predictive applications. This method divides a dataset into two subsets, one for training and the other for validation. The analysis is performed on the training data, and the results are validated using the validation data. To reduce data scattering, the cross-validation process is repeated several times using different sets, and the average of the validation results is used as the final output. Other testing and training methodologies

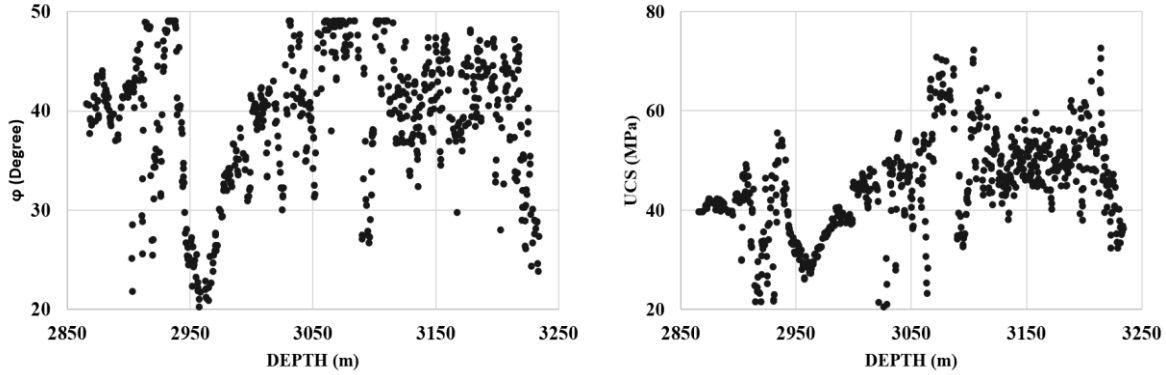

Fig. 7 Scatter plots of the target variables versus depth

include Leave-one-out, Leave-P-out, and K-fold techniques. In this particular study, the cross-validation method was utilized. Fig. 6 shows the flowchart for the suggested numerical methods in this research.

As Fig. 6 explains, this research proposes a cross-validation method to evaluate the process and predict the response of residual changes. We introduce an approach we refer to as nested cross-validation (NCV). To begin, we randomly divided the dataset into two subsets: 70% for training and 30% for testing, as illustrated in the flowchart in Figure 6. Next, we further split the training dataset into two parts: 70% for estimating the trend and 30% for validating it. In the subsequent phase, we utilize the Trend training dataset to explore a variety of initial parameters for our proposed methods. By fitting the model to this dataset using the input variables Vp and Vs, we aim to determine the optimal parameters for the MARS, Ridge, and Lasso methods, denoted as $\hat{\beta}^{MARS}$ ،$\hat{\beta}^{Ridge}$, $\hat{\beta}^{Lasso}$, respectively. These optimal parameters are identified based on the minimum Mean Squared Prediction Error (MSPE), which we calculate as the mean of the squared differences between the estimated values using detrending methods and the Trend test data. Following this, we use the optimal parameters obtained to fit the model with the input variables to the response variable data of the Total test set. The estimated values for the three aforementioned methods are depicted in Fig. 6 as $\hat{f}^{MARS}$ ،$\hat{f}^{Ridge}$ و $\hat{f}^{Lasso}$ Afterward, we calculate the residuals by subtracting the estimated values from the previous step from the actual response variable data of the Total test set. To proceed with forecasting using geostatistical methods, particularly ordinary Kriging (OK), we emphasize the importance of selecting an appropriate variogram model. We visually assess the experimental variogram curves and determine that the exponential model provides the best fit for all three methods. Next, we apply ordinary Kriging to the remaining values of the Total test set. The predicted values of the Total test residuals are displayed in Fig. 6 as $\hat{\sigma}$. Finally, we obtain the predictions of the response variables φ and UCS for the Total test set. These predictions are derived from the sum of the trend estimate ($\hat{f}$) and the predicted values obtained from ordinary Kriging applied to the corresponding residuals ($\hat{\sigma}$) all at the same level.

Table 1 GCV report and optimal parameters of Lasso and Ridge

Method	MARS	Lasso	Ridge
Parameter	GCV	$\hat{\beta}^{Lasso}$	$\hat{\beta}^{Ridge}$
φ	18.51	0.0082	0.4607
UCS	6.43	0.0692	0.9584

5. Results and discussion

Here, the ordinary Kriging is performed by modeling the trends of MARS, Lasso, and Ridge for the data of two variables: UCS and φ. The scatter plot of the studied variables concerning the depth is shown in Fig 7.

The graphs clearly show trends in the data plots. Hence, the data must be separated from any trends. Before initiating this stage, we used cross-validation of two randomly chosen data sets (70%) training and (30%) testing data set. The training data based on MSPE selects the optimal model.

To select the optimal model fitted to the trend, we again randomly divided the training set into two sets the trend training set (70%) and the trend test set (30%). We fitted the models from the proposed methods to the trend training set and obtained the optimal parameters based on the MSPE criterion. The optimal parameter of each model is obtained from the mean of the squared differences of the estimated value of the target variable at the new location. x_{new} and the corresponding real value in the trend test set. The optimal parameters of the three regression models are presented in Table 1.

We optimized the model and estimated the fitting trend of the test data. Regression models obtained from the three methods of MARS, Lasso, and Ridge are presented in Eqs. (11.1), (11.2), and (11.3), respectively. In (11.1a), the trend of variable φ is estimated using the MARS method and is reported to include the intercept and eight basis functions and their corresponding regression coefficients. For Estimating trend φ, the MARS method uses the observations of both Vp and Vs. Variables.

In contrast, estimating the trend of the UCS variable has only the intercept and two basic functions and uses the Vp observations (11.1b). Also, the Lasso method uses the Vp

Table 2 The final results for UCS and φ prediction by MARS, Lasso, and Ridge

Benchmark	MSPE		R^2		MAPE		MBPE	
Parameter/Method	φ	UCS	φ	UCS	φ	UCS	φ	UCS
MARS	2.64	7.11	0.97	0.96	0.97	1.55	0.04	0.16
Lasso	2.71	9.83	0.97	0.95	0.99	1.78	-0.01	0.14
Ridge	2.29	8.17	0.98	0.95	0.91	1.64	-0.00	0.16

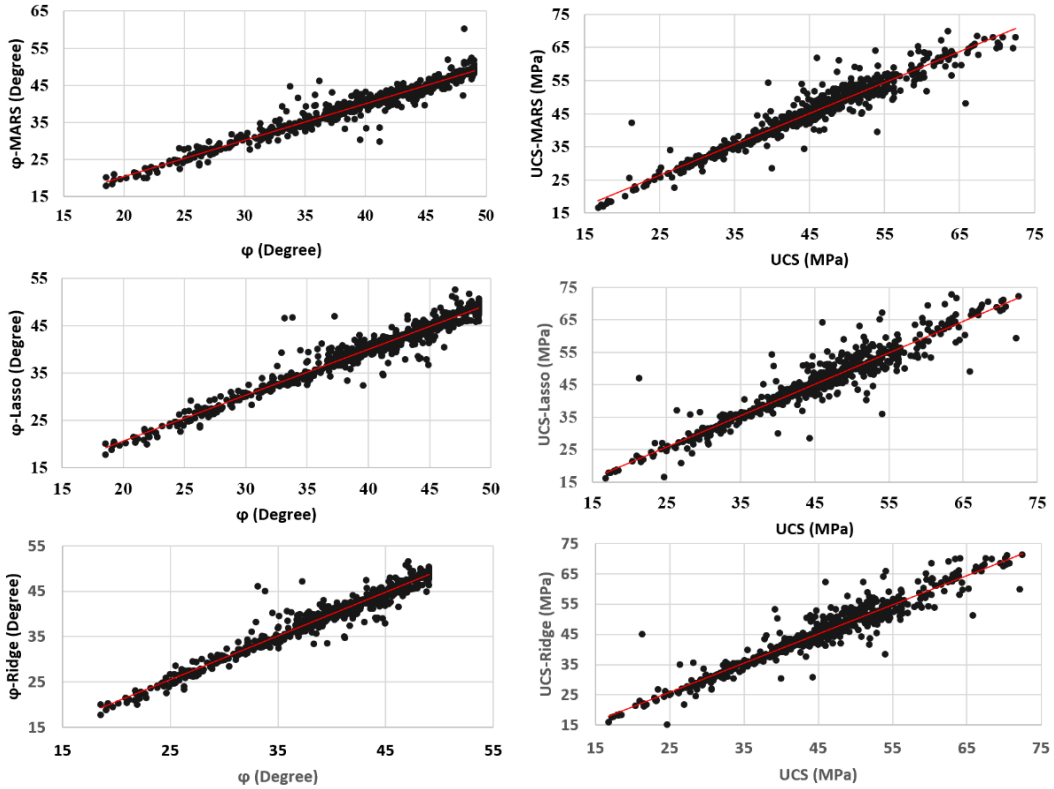

Fig. 8 Scatter plots of predicted values versus actual test data values using MARS-ordinary Kriging of the first row, Lasso-ordinary Kriging of the second row, and third-order Ridge-ordinary Kriging for the target variables φ and UCS

and Vs to model the trend of φ (11.2a), yet similar to the MARS model, it only uses the Vp observations for UCS. (11.2b).

$$\hat{f}_{\varphi}^{MARS}(X) = 32.98 + 0.01 * (V_P - 4189.78)_+ - 0.01 * (4757.6 - V_P)_+ - 0.02 * (V_P - 4757.64)_+ + 0.02 * (V_P - 4889)_+ - 0.01 * (V_P - 5144.9)_+ + 0.02 * (2064.43 - V_S)_+ + 0.01 * (V_S - 2245)_+ - 0.01 * (V_S - 3132.9)_+ \quad (11.1a)$$

$$\hat{f}_{UCS}^{MARS}(X) = 36.62 - 0.012 * (4430.09 - V_P)_+ + 0.02 * (V_P - 4430.09)_+ \quad (11.1b)$$

As stated before, the Ridge approach does not apply the

$$\hat{f}_{\varphi}^{Lasso}(X) = 3.61 + 0.009 * V_P - 0.002 * V_S \quad (11.2a)$$

$$\hat{f}_{UCS}^{Lasso}(X) = -30.77 + 0.01 * V_P \quad (11.2b)$$

$$\hat{f}_{\varphi}^{Ridge}(X) = 5.13 + 6.98 * 10^{-3} * V_P + 5.47 * 10^{-5} * V_S \quad (11.3a)$$

$$\hat{f}_{UCS}^{Ridge}(X) = -26.51 + 0.012 * V_P + 0.004 * V_S \quad (11.3b)$$

variable selection, and it's fitting trend is presented in Eqs. (11.3a and 11.3b). After detrending the data, we calculated the residuals from the models by running the ordinary Kriging on the residuals obtained from the three mentioned methods. The results of the cross-validation of the test data prediction (the sum of the estimation of the trend and the value of the residuals of the test set) were predicted using ordinary Kriging and reported in Fig. 8.

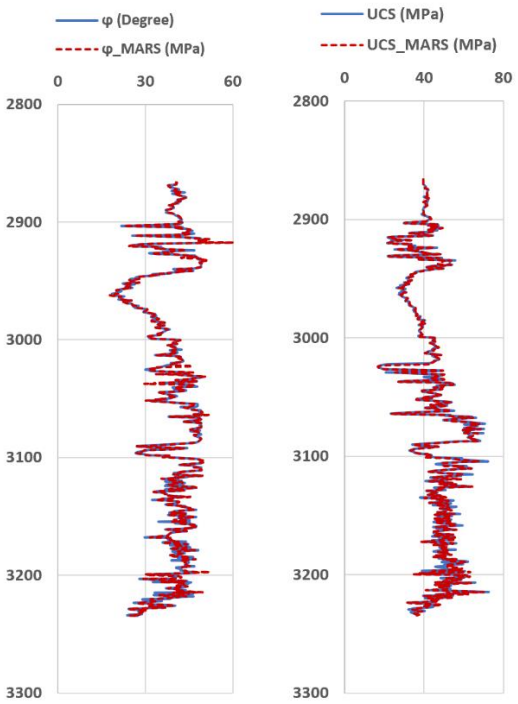

Fig. 9 Well-logging curves of the prediction results by the MARS method

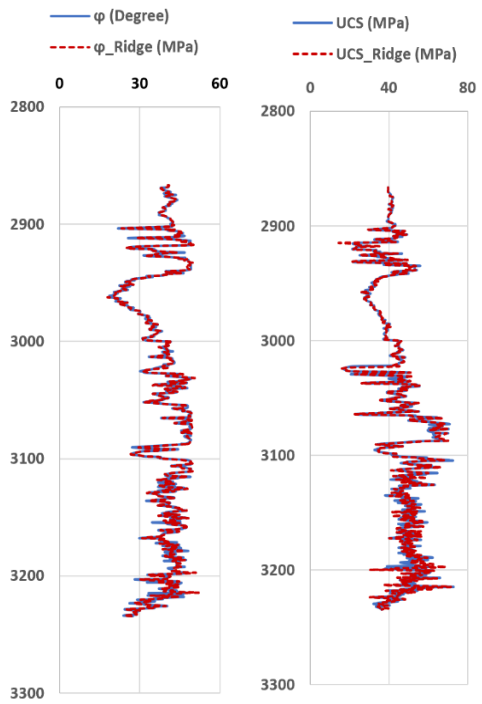

Fig. 11 Well-logging curves of the prediction results by the Ridge method

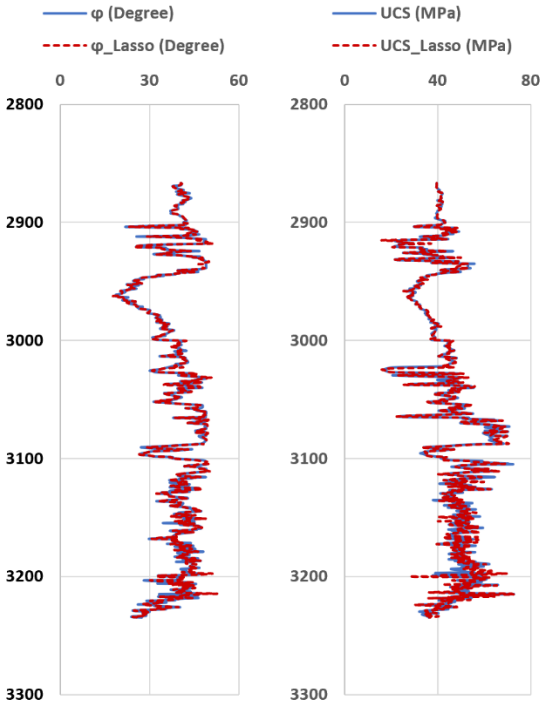

Fig. 10 Well-logging curves of the prediction results by the Lasso method

According to the graphs, it can be concluded that the data distribution is approximately revolving around the bisector of the first and third quadrants, which indicates the appropriateness of the proposed methods. Also, the MSPE, R^2, MAPE, and MBPE are calculated and reported in Table 2.

Based on the values in the table, for the variable φ, the Ridge method has performed better spatial prediction than the Lasso and MARS methods. It also has the lowest MSPE and the highest R^2 values. In addition, the MAPE shows the lowest value, and the MBPE is closest to Zero. Therefore, the values mentioned earlier also approve the better application of the Ridge method. Also, for the variable UCS, the MARS method has the lowest value of MSPE and MAPE and the highest value of R^2, Which shows the better performance of this method compared to other methods. Well-logging of the prediction results is available in Figs. 9 to 11.

6. Conclusions

Building reliable spatial analysis and prediction models in various applied situations, including geoscience applications and oil drilling, remains a complex task that requires effective approaches and techniques. This study highlighted the potential of machine learning and geostatistical techniques for enhancing the accuracy and efficiency of predicting rock mechanical properties. The approach relies solely on seismic velocity measurements routinely generated in subsurface investigations. This makes it practical and applicable for a wide range of subsurface studies. Overall, the proposed methodology provides a new avenue for accurately characterizing the geomechanical properties of rocks. Geostatistical methods and trend function modeling using three machine learning techniques, namely MARS, Ridge, and Lasso regression, were implemented on the data to predict rocks' internal friction angle (φ) and uniaxial compressive strength (UCS).

The findings indicate the superiority of the MARS and Ridge methods in estimating the trend functions and spatially predicting the target variables compared to the Lasso method. For the variable φ, the Ridge model performed better with the lowest MSPE and highest R^2 values, while for the variable UCS, the MARS model performed better with the lowest MSPE and MAPE and the highest R^2.

These results demonstrate that integrating machine learning techniques with geostatistical methods can provide effective solutions for modeling and predicting geospatial variables. With effective trend modeling and Kriging of residuals, accurate geospatial predictions can be achieved, with low prediction errors and high accuracy, to aid subsurface studies and applications, as indicated by the cross-validation metrics.

Acknowledgments

The paper's authors express a special thanks to the dear associate editor and reviewers for investigating the technicality of the manuscript.

References

Abd El Aal, A., Al Zamana, Y., Dunquwah, T., Alsalmi, O., Hussain, J., Iqbal, J. and AL-AWAH, H.E.Z.A.M. (2025), "Depth variations as effective indicators for strength variation of Najran granites, Najran Region, Saudi Arabia", *Front. Mater.*, **11**, 1382313. https://doi.org/10.3389/fmats.2025.1382313.

Abdullah, G.M., Abd El Aal, A., Al Saiari, M. and Radwan, A.E. (2023a), "Sustainable impact of Coarse Aggregate Crushing Waste (CACW) in decreasing carbon footprint and enhancing geotechnical properties of silty sand soil", *Appl. Sci.*, **13**(19), 10930. https://doi.org/10.3390/app131910930.

Abdullah, G.M., El-Aal, A.A., Radwan, A.E. and Al-Awah, H. (2023b), "Numerical simulation and diagnosis geotechnical parameters of historical buildings in Najran City, Kingdom of Saudi Arabia", *Scientific Reports*, **13**(1), 16968. https://doi.org/10.1038/s41598-023-439591.

Al-Homidy, A.A., Abd El Aal, A.K., Nabawy, B.S. and Radwan, A.E. (2024), "Effect of adding cement kiln dust on the effective geotechnical properties of sand dunes in Najran–Sharourah, Kingdom of Saudi Arabia: a laboratory study", *J. Mater. Cycles Waste Management*, **26**(1), 373-391. https://doi.org/10.1007/s10163-023-01831-4.

Cressie, N. (1991), *Geostatistical Analysis of Spatial Data. Spatial Statistics And Digital Image Analysis*, National Academy Press, Washington, D.C, USA.

Cressie, N. (2015), *Statistics for Spatial data*, John Wiley & Sons, NewYork, USA.

Cressie, N. and Moores, M.T. (2022), *Spatial statistics. In Encyclopedia of Mathematical Geosciences*, Springer International Publishing, Cham, Switzerland.

Dong, Z., Li, Y., Li, H., Shi, X., Ma, H., Zhao, K. and Zhao, A. (2022), "Influence of loading history on creep behavior of rock salt", *J. Energy Storage*, **55**, 105434. https://doi.org/10.1016/j.est.2022.105434.

Elyasi, A. and Goshtasbi, K. (2015), "Using different rock failure criteria in wellbore stability analysis", *Geomech. Energ. Environment*, **2**, 15-21. https://doi.org/10.1016/j.gete.2015.04.001.

Elyasi, A., Goshtasbi, K. and Hashemolhosseini, H. (2016), "A coupled geomechanical reservoir simulation analysis of CO2-EOR: a case study", *Geomech. Eng.*, **10**(4), 423-436. https://doi.org/10.12989/gae.2016.10.4.423.

Elyasi, A., Makarian, E. and Saberi, F. (2023), "Fracture gradient prediction: Applicable to safe drilling and underground storage operations", *Proceedings of the 7th International Conferences on Applied Research in Science and Engineering*, London, United Kingdom, May.

Farhadian, A., Ghasemi, E., Hoseinie, S.H. and Bagherpour, R. (2022), "Prediction of rock abrasivity index (RAI) and uniaxial compressive strength (UCS) of granite building stones using nondestructive tests", *Geotech. Geol. Eng.*, **40**(6), 3343-3356 https://doi.org/10.1007/s10706-022-02095-9.

Friedman, J.H. and Stuetzle, W. (1981), "Projection pursuit regression", *J. Am. Stat. Association*, **76**(376), 817-823. https://doi.org/10.1080/01621459.1981.10477729

Gao, H., Wang, Q., Jiang, B., Zhang, P., Jiang, Z. and Wang, Y. (2021), "Relationship between rock uniaxial compressive strength and digital core drilling parameters and its forecast method", *Int. J. Coal Science & Technology*, **8**(4), 605-613. https://doi.org/10.1007/s40789-020-00383-4

Goshtasbi, K., Elyasi, A., & Naeimipour, A. (2013), "3D numerical stability analysis of multi-lateral well junctions", *Arabian Journal of Geosciences*, **6**, 2981–2989. https://doi.org/10.1007/s12517-012-0558-x

Hashemi, R., Saberi, F., Asoude, P. and Soleimani, B. (2024), "Enhancing reservoir zonation through triple porosity system: A case study", *SPE J.*, **29**(6), 3043-3062. https://doi.org/10.2118/219491-PA

Hastie, T., Tibshirani, R., Friedman, J.H. and Friedman, J.H. (2009), *The Elements of Statistical Learning: Data Mining, Inference, And Prediction*, Springer Publication, New York, USA.

Hengl, T., Heuvelink, G. B., & Rossiter, D. G. (2007)," About regression-kriging: From equations to case studies", *Comput. Geosci.*, **33**(10), 1301-1315. https://doi.org/10.1016/j.cageo.2007.05.001

Hernomita, D. and Erfando, T. (2023), "Sensitivity analysis of geomechanics influence on the success of hydraulic fracturing in shale gas reservoir", *J. Geosci., Eng. Environ. Tech.*, **8**(2), 99-104. https://doi.org/10.25299/jgeet.2023.8.2.12351.

Hudson, J.A. and Harrison, J.P. (2000), *Engineering Rock Mechanics: An Introduction to The Principles*, Elsevier Publication, Oxford, UK.

Isah, B.W., Mohamad, H., Ahmad, N.R., Harahap, I.S.H. and Al-Bared, M.A.M. (2020), "Uniaxial compression test of rocks: Review of strain measuring instruments", *In IOP Conference Series: Earth and Environmental Science*, Kedah, Malaysia, November.

James, G., Witten, D., Hastie, T. and Tibshirani, R. (2013), *An Introduction to Statistical Learning*, Springer ,New York, USA.

Johnston, R., Jones, K. and Manley, D. (2018), "Confounding and collinearity in regression analysis: a cautionary tale and an alternative procedure, illustrated by studies of British voting behaviour", *Quality and Quantity*, **52**, 1957-1976. https://doi.org/10.1007/s11135-017-0584-6.

Karaman, K. (2024). "The effect of in-situ stress parameters and metamorphism on the geomechanical and mineralogical behavior of tunnel rocks", *Geomech. Eng*., **37**(3), 213-222. https://doi.org/10.12989/gae.2024.37.3.213

Karev, V., Kovalenko, Y. and Ustinov, K. (2020), "*Geomechanics of Oil and Gas Wells*, Springer Cham, Cham, Switzerland.

Khalifeh-Soltani, A., Alavi, S.A., Ghassemi, M.R. and Ganjiani, M. (2021), "Geomechanical modelling of fault-propagation folds: estimating the influence of the internal friction angle and friction coefficient", *Tectonophysics*, **815,** 228992.

https://doi.org/10.1016/j.tecto.2021.228992.

Labuz, J.F. and Zang, A. (2012), The *ISRM Suggested Methods for Rock Characterization, Testing and Monitoring*, Springer, Cham, Switzerland.

Larki, E., Jaffarbabaei, B., Soleimani, B., Elyasi, A., Saberi, F., Makarian, E. and Radwan, A.E. (2023), "A new insight to access carbonate reservoir quality using quality factor and velocity deviation log", *Acta Geophysica*, **71**(6) 1-20. https://doi.org/10.1007/s11600-023-01249-4.

Lee, M.G., Kim, Y., Cho, H.I., Kim, H.S., Sun, C.G., Seong, Y.J., and Che, I.Y. (2024), "KIGAM Quake: An open platform for seismological data and earthquake research information", *Geomech. Eng.*, **37**(3), 279-291. https://doi.org/10.12989/gae.2024.37.3.279.

Liu, H.Y., Han, H., An, H.M. and Shi, J.J. (2016), "Hybrid finite-discrete element modelling of asperity degradation and gouge grinding during direct shearing of rough rock joints", *Int. J. Coal Sci. Tech.*, **3**, 295-310. https://doi.org/10.1007/s40789-016-0142-1.

Makarian, E., Abad, A.B.M.N., Manaman, N.S., Mansourian, D., Elyasi, A., Namazifard, P. and Martyushev, D.A. (2023a), "An efficient and comprehensive poroelastic analysis of hydrocarbon systems using multiple data sets through laboratory tests and geophysical logs: a case study in an Iranian hydrocarbon reservoir", *Carbonates and Evaporites*, **38**(2), 295-310. https://doi.org/10.1007/s40789-016-0142-1

Makarian, E., Elyasi, A., Moghadam, R.H., Khoramian, R. and Namazifard, P. (2023b), "Rock physics-based analysis to discriminate lithology and pore fluid saturation of carbonate reservoirs: a case study", *Acta Geophysica*, **71**(5), 2163-2180. https://doi.org/10.1007/s11600-023-01029-0.

Makarian, E., Mirhashemi, M., Elyasi, A., Mansourian, D., Falahat, R., Radwan, A.E., El-Aal, A., FanLi, D. and Li, H. (2023c), "A novel directional-oriented method for predicting shear wave velocity through empirical rock physics relationship using geostatistics analysis", *Scientific Reports,* **13**(1), 19872. https://doi.org/10.1038/s41598-023-47016-9.

McDonald, G.C. (2009), "Ridge regression", *Wiley Interdisciplinary Reviews: Computational Statistics*, **1**(1), 93-100. https://doi.org/10.1002/wics.14.

Min, D.H. and Yoon, H.K. (2024), "Prediction of dynamic soil properties coupled with machine learning algorithms", *Geomech. Eng.*, **37**(3), 253-262. https://doi.org/10.12989/gae.2024.37.3.253

Min, G., Fukuda, D., Oh, S., Kim, G., Ko, Y., Liu, H. and Cho, S. (2020), "Three-dimensional combined finite-discrete element modeling of shear fracture process in direct shearing of rough concrete–rock Joints", *Appl. Sci.*, **10**(22), 8033. https://doi.org/10.3390/app10228033.

Mirhashemi, M., Khojasteh, E.R., Manaman, N.S. and Makarian, E. (2022), "Efficient sonic log estimations by geostatistics, empirical petrophysical relations, and their combination: Two case studies from Iranian hydrocarbon reservoirs', *J. Petroleum Sci. Eng.*, **213**, 110384. https://doi.org/10.1016/j.petrol.2022.110384.

Munjiza, A.A. (2004), *The Combined Finite-Discrete Element Method*, John Wiley & Sons, Hoboken, New Jersey, USA.

Saberi, F. and Hosseini-Barzi, M. (2024), "Effect of thermal maturation and organic matter content on oil shale fracturing", *Int. J. Coal Sci. Tech.*, **11**(1), 1-19. https://doi.org/10.1007/s40789-024-00666-0.

Sadeghi, E., Nikudel, M.R., Khamehchiyan, M. and Kavussi, A. (2022), "Estimation of unconfined compressive strength (UCS) of carbonate rocks by index mechanical tests and specimen size properties: central Alborz Zone of Iran", *Rock Mech. Rock Eng.*, **55**(1), 125-145, https://doi.org/10.1007/s00603-021-02532-w.

Shouri, H., Shahbazi, K. and Abdideh, M. (2024), "Development of one-dimensional and three-dimensional geomechanical modeling of reservoir rock in oil fields", *Model. Earth Syst. Environ.*, **10**(2), 2271-2294. https://doi.org/10.1007/s40808-023-01907-y.

Tsoi, P. and Usol'tseva, O. (2019), "Comparative analysis of Cohesion Coefficient and International friction angels of rocks depending the functional type of the mohr-couobm envelope", *Int. Multidisciplinary Scientific Geo Conference: SGEM*, **19**(1.3), 119-126. https://doi.org/10.5593/sgem2019/1.3.

Villeneuve, M.C. and Heap, M.J. (2021), "Calculating the cohesion and internal friction angle of volcanic rocks and rock masses", *Volcanica,* **4**(2), 279-293. https://doi.org/10.30909/vol.04.02.279293.

Wang, H. and He, M. (2023), "Determining method of tensile strength of rock based on friction characteristics in the drilling process", *Rock Mech. Rock Eng.*, **56**(6), 4211-4227. https://doi.org/10.1007/s00603-023-03276-5.

Xu, M. and Jin, D. (2024), "Prediction of the long-term deformation of high rockfill geostructures using a hybrid back-analysis method", *Geomech. Eng.*, **36**(1), 83-97. https://doi.org/10.12989/gae.2024.36.1.083.

Zhang, D., Ranjith, P.G. and Perera, M.S.A. (2016), "The brittleness indices used in rock mechanics and their application in shale hydraulic fracturing: A review", *J. Petroleum Ssci. Eng.*, **143**, 158-170. https://doi.org/10.1016/j.petrol.2016.02.011.

Zhou, H., Chen, J., Lu, J., Jiang, Y. and Meng, F. (2018), "A new rock brittleness evaluation index based on the internal friction angle and class I stress–strain curve", *Rock Mech. Rock Eng.*, **51**, 2309-2316. https://doi.org/10.1007/s00603-018-1487-0.

Zoback, M.D. and Kohli, A.H. (2019), *Unconventional Reservoir Geomechanics*, Cambridge University Press, Cambridge, England.

CC